THE ASTROPHYSICAL JOURNAL, 557:1021–1027, 2001 August 20

PRELIMINARY CONSTRAINTS ON $^{12}C(\alpha, \gamma)^{16}O$ FROM WHITE DWARF SEISMOLOGY

T. S. METCALFE,[1,2] D. E. WINGET,[1] AND P. CHARBONNEAU[3]

Received 2001 February 21; accepted 2001 April 11

ABSTRACT

For many years, astronomers have promised that the study of pulsating white dwarfs would ultimately lead to useful information about the physics of matter under extreme conditions of temperature and pressure. In this paper, we finally make good on that promise. Using observational data from the Whole Earth Telescope and a new analysis method employing a genetic algorithm, we empirically determine that the central oxygen abundance in the helium-atmosphere variable white dwarf GD 358 is 84% ± 3%. We use this value to place preliminary constraints on the $^{12}C(\alpha, \gamma)^{16}O$ nuclear reaction cross section. More precise constraints will be possible with additional detailed simulations. We also show that the pulsation modes of our best-fit model probe down to the inner few percent of the stellar mass. We demonstrate the feasibility of reconstructing the internal chemical profiles of white dwarfs from asteroseismological data and find an oxygen profile for GD 358 that is qualitatively similar to recent theoretical calculations.

Subject headings: methods: numerical — nuclear reactions, nucleosynthesis, abundances — stars: individual (GD 358) — stars: interiors — stars: oscillations — white dwarfs

1. INTRODUCTION

White dwarf stars are the endpoints of stellar evolution for the majority of all stars, and their composition and structure can tell us about their prior history. Compared to main-sequence stars, white dwarfs are relatively simple objects to model. Once they pass through the hot planetary nebula nucleus phase, their evolution is a slow cooling process largely uncomplicated by nuclear burning or other poorly understood effects. Nature has been kind by providing several varieties of otherwise normal white dwarf stars that undergo continuous and remarkably stable pulsations. We can determine the internal structure of these pulsating white dwarfs by observing their variations in brightness over time and then matching these observations with a computer model that behaves the same way.

In the past decade, the observational aspects of white dwarf seismology have been addressed by the development of the Whole Earth Telescope (Nather et al. 1990). This instrument is now mature and has provided a wealth of seismological data on the different varieties of pulsating white dwarf stars. In an effort to bring the analytical treatment of these data to a comparable level of sophistication, we have recently developed an objective global optimization method for white dwarf pulsation models based on a genetic algorithm (see § 2 of Metcalfe, Nather, & Winget 2000 and references therein for a detailed discussion of genetic algorithms). Metcalfe et al. (2000) applied this new approach to observations of the helium-atmosphere variable white dwarf GD 358, allowing the stellar mass (M_*), the effective temperature ($T_{\rm eff}$), and the mass of the surface helium layer ($M_{\rm He}$) to be free parameters. They repeated the procedure for several combinations of core composition and internal chemical profiles. Among other things, this initial study demonstrated that the fits were significantly improved by searching globally with different core compositions. The obvious next step is to extend this method to treat the central oxygen abundance as a free parameter. This has the exciting potential to allow us to place meaningful constraints on the $^{12}C(\alpha, \gamma)^{16}O$ nuclear reaction cross section.

The value of the $^{12}C(\alpha, \gamma)^{16}O$ cross section at stellar energies is presently the result of an extrapolation across 8 orders of magnitude from laboratory data (Fowler 1986). During the final stages of a red giant star, this reaction competes with the triple-α process for the available α-particles. As a consequence, the final ratio of carbon to oxygen in the core of a white dwarf is a measure of the relative rates of the two reactions (Buchmann 1996). The triple-α reaction is relatively well determined at the relevant energies, so the constraint that comes from this measurement is much more precise than other methods.

2. FORWARD MODELING

The initial three-parameter fits to GD 358 (Metcalfe et al. 2000, hereafter MNW) made it clear that both the central oxygen abundance and the shape of the internal chemical profile should be treated as free parameters. We modified our code to allow any central oxygen mass fraction ($X_{\rm O}$) between 0.00 and 1.00 with a resolution of 1%. To explore different chemical profiles, we fixed $X_{\rm O}$ to its central value out to a fractional mass parameter (q) that varied between 0.10 and 0.85 with a resolution of 0.75%. From this point, we forced $X_{\rm O}$ to decrease linearly in mass to zero oxygen at the 95% mass point.

This parameterization is a generalized form of the "steep" and "shallow" profiles used in Metcalfe et al. (2000). We originally used these profiles so that our results could be easily compared with earlier work by Wood (1990) and Bradley, Winget, & Wood (1993). The latter authors define both profiles in their Figure 1. The shallow profile corresponds to approximately $q = 0.5$, and the steep to roughly $q = 0.8$. However, in our generalized parameterization, we have moved the point where the oxygen

[1] Department of Astronomy, Mail Code C1400, University of Texas at Austin, Austin, TX 78712; travis@astro.as.utexas.edu, dew@astro.as.utexas.edu.

[2] Visiting Scientist, High Altitude Observatory, National Center for Atmospheric Research.

[3] High Altitude Observatory, National Center for Atmospheric Research, P.O. Box 3000, Boulder, CO 80307; paulchar@hao.ucar.edu.

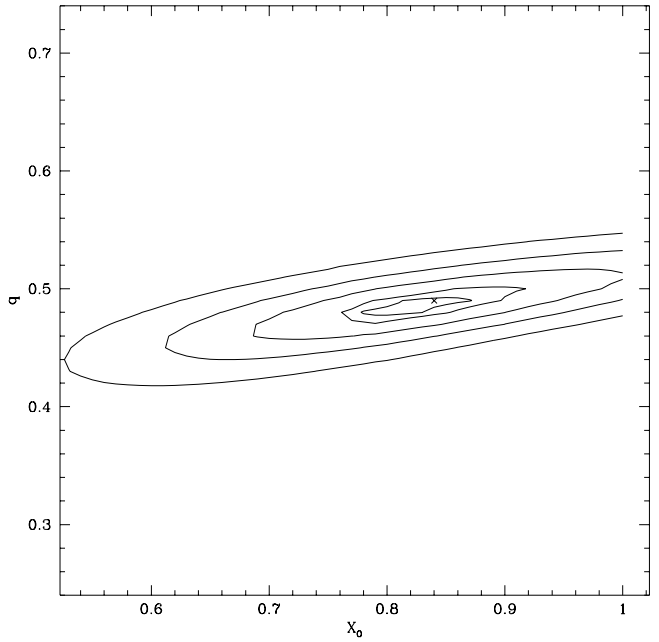

FIG. 1.—Contour plot of the central oxygen mass fraction (X_O) vs. the fractional mass location of the change in the oxygen gradient (q) with M_*, T_{eff}, and M_{He}/M_* fixed at their best-fit values. The model with the absolute minimum residuals (identical to the best fit found by the GA) is marked with a cross. The contours are drawn at 1, 3, 10, 25, and 40 times the observational noise.

abundance goes to zero from a fractional mass of 0.9 out to a fractional mass of 0.95. This coincides with the boundary in our models between the self-consistent core and the envelope, where we describe the He-C transition using a diffusion equilibrium profile from the method of Arcoragi & Fontaine (1980) with diffusion exponents of ± 3. We do not presently include oxygen in the envelopes, so the mass fraction of oxygen must drop to zero by this point.

We calculated the magnitude of deviations from the mean period spacing for models using our profiles and compared them with those using smooth profiles from recent theoretical calculations by Salaris et al. (1997). The smooth theoretical profiles caused significantly larger deviations. Therefore, we conclude that the abrupt changes in the oxygen abundance resulting from our parameterization do not have an unusually large effect on the period spacing (see Appendix for details). Although the actual chemical profiles will almost certainly differ from the profiles resulting from our simple parameterization, we should still be able to probe the gross features of the interior structure by matching one or another linear region of the presumably more complicated physical profiles.

We used the same ranges and resolution for M_*, T_{eff}, and M_{He} as those used in MNW, so the search space for this five-parameter problem is 10,000 times larger than for the three-parameter case. Initially, we tried to vary all five parameters simultaneously, but this proved to be impractical because of the parameter degeneracy between M_* and q. The pulsation properties of the models depend on the *radial* location in the chemical profile where the oxygen mass fraction begins to change. If the genetic algorithm (GA) finds a combination of M_* and q that yields a reasonably good fit to the data, most changes to either one will not, by themselves, improve the fit. As a consequence, simultaneous changes to both parameters are required to find a better fit, and since this is not very probable, the GA must run for a very long time. Tests on synthetic data for the full five-parameter problem yielded only a 10% probability of finding the input model, even when we ran for 2000 generations—10 times longer than for the three-parameter case. By contrast, when we used a fixed value of q and repeated the test with only four free parameters, the GA found the input model in only 400 generations for eight out of 10 runs. Even better, by fixing the mass and allowing q to vary, it took only 250 generations to find the input model in seven out of 10 runs. This suggests that it might be more efficient to alternate between these two subsets of four parameters, fixing the fifth parameter each time to its best-fit value from the previous iteration, until the results of both fits are identical.

Since we do not know a priori the precise mass of the white dwarf, we need to ensure that this iterative four-parameter approach will work even when the mass is initially fixed at an incorrect value. To test this, we calculated the pulsation periods of the best-fit 0.65 $M_\odot$ model for GD 358 from MNW [$T_{eff} = 22{,}600$ K, $\log (M_{He}/M_*) = -2.74$, 20:80 C/O shallow] and then iteratively applied the two four-parameter fitting routines, starting with the mass fixed at 0.60 $M_\odot$—a difference comparable to the discrepancy between the mass found by MNW and the value found by Bradley & Winget (1994). The series of fits leading to the input model is shown in Table 1. This method required only three iterations, and for each iteration we performed 10 runs with different random initialization to yield a probability of finding the best fit much greater than 99.9%. In the end, the method required a total of 2.5×10^6 model evaluations (128 trials per generation, 10 runs of 650 generations per iteration). This is about 200 times more efficient than calculating the full grid in each iteration, and about 4000 times more efficient than a grid of the entire five-dimensional space.

Next, we applied this method to the observed pulsation periods of GD 358. We initially fixed the mass at 0.61 $M_\odot$, the value inferred from the original asteroseismological study by Bradley & Winget (1994). The solution converged after four iterations, and the best-fit values of the five parameters were

$$T_{eff} = 22{,}600 \text{ K}\,, \quad M_* = 0.650\ M_\odot\,,$$
$$\log (M_{He}/M_*) = -2.74\,, \quad X_O = 0.84\,, \quad q = 0.49\,.$$

Note that the values of M_*, T_{eff}, and M_{He} are identical to those found in MNW. The best-fit mass and temperature still differ significantly from the values inferred from spectroscopy by Beauchamp et al. (1999). However, the luminosity of our best-fit model is consistent with the luminosity derived from the measured parallax of GD 358 (Harrington et al. 1985).

TABLE 1

CONVERGENCE OF METHOD ON SYNTHETIC DATA

Iteration	T_{eff} (K)	M_* ($M_\odot$)	$\log(M_{He}/M_*)$	X_O	q
1[a]	23,600	0.600	−5.76	0.52	0.55
1[b]	22,200	0.660	−2.79	0.99	0.55
2[a]	22,200	0.660	−2.79	0.88	0.51
2[b]	22,600	0.650	−2.74	0.85	0.51
3[a]	22,600	0.650	−2.74	0.80	0.50
3[b]	22,600	0.650	−2.74	0.80	0.50

[a] Value of M_* fixed during this iteration.
[b] Value of q fixed during this iteration.

To alleviate any doubt that the GA had found the best combination of X_O and q and to obtain a more accurate estimate of the uncertainties on these parameters, we calculated a grid of 10,000 models with the mass, temperature, and helium-layer mass fixed at their best-fit values. A contour plot of this grid near the solution found by the GA is shown in Figure 1.

3. REVERSE APPROACH

The results of forward modeling with one adjustable point in the chemical profile make it clear that information about the internal structure is contained in the data, and that we simply need to learn how to extract it. If we want to test more complicated adjustable profiles, forward modeling quickly becomes too computationally expensive as the dimensionality of the search space increases. We need to devise a more efficient approach to explore the myriad possibilities.

The natural frequency that dominates the determination of pulsation periods in white dwarf models is the Brunt-Väisälä (B-V) frequency, which we calculate using the Modified Ledoux treatment described in Tassoul, Fontaine, & Winget (1990). To get a sense of how the pulsation periods depend on the B-V frequency in various regions of the model interior, we added a smooth perturbation to the best-fit model of GD 358 from MNW, moving it one shell at a time from the center to the surface. The perturbation artificially decreased the B-V frequency across seven shells, with a maximum amplitude of 10%. We monitored the effect on each of the pulsation periods as the perturbation moved outward through the interior of the model. The results of this experiment for the pulsation periods corresponding to those observed in GD 358 are shown in Figure 2. Essentially, this experiment demonstrates that the pulsation periods are sensitive to the conditions all the way down to the inner few percent of the model. Since the observational uncertainties on each period are typically only a few hundredths of a second, even small changes to the B-V frequency in the model interior are significant.

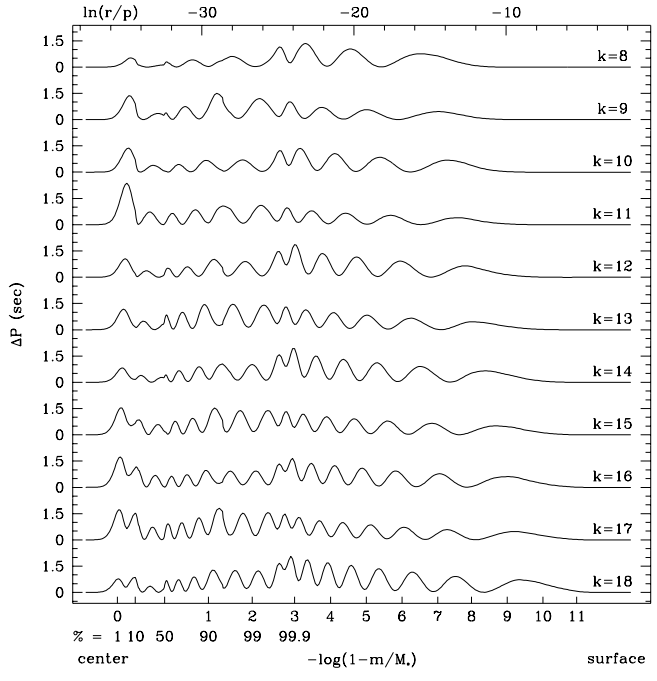

FIG. 2.—For the best-fit model of GD 358 from Metcalfe et al. (2000), the change in pulsation period is shown for $l = 1$ modes of various radial overtone number (k) that result from a smooth artificial 10% decrease in the Brunt-Väisälä frequency as a function of the natural logarithm of the ratio of the distance from the center of the model to the local pressure (*top axis*) and the fractional mass coordinate $-\log(1 - m/M_*)$ (*bottom axis*). The center of the model is to the left and the surface is to the right. Also indicated is the mass fraction expressed as a percentage for several values closer to the center.

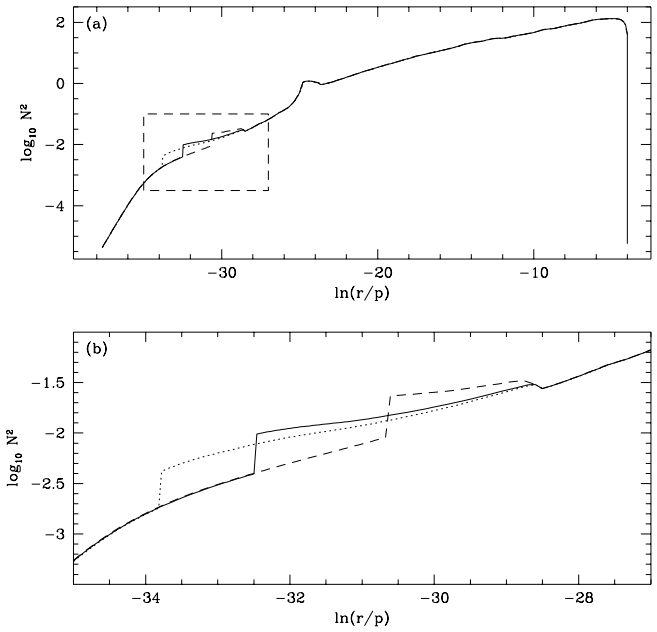

FIG. 3.—The Brunt-Väisälä frequency as a function of the radial coordinate $\ln(r/p)$ for several models with the same mass, temperature, helium-layer mass, and central oxygen mass fraction but different internal chemical profiles (*a*) from the center of the model at left to the surface at right, and (*b*) only in the range of $\ln(r/p)$ indicated by the dashed box in the upper panel. The three curves correspond to a profile with q equal to 0.2 (*dotted line*), 0.49 (*solid line*), and 0.8 (*dashed line*).

The rms residuals between the observed pulsation periods in GD 358 and those calculated for the best fit from forward modeling are still much larger than the observational noise. This suggests that either we have left something important out of our model or we have neglected to optimize one or more of the parameters that could, in principle, yield a closer match to the observations. To investigate the latter possibility, we introduced ad hoc perturbations to the B-V frequency of the best-fit model to see if the match could be improved. Initially, we concentrated on the region of the Brunt-Väisälä curve that corresponds to the internal chemical profile.

If we look at the B-V frequency for models with the same mass, temperature, helium-layer mass, and central oxygen mass fraction but with different internal chemical profiles (see Fig. 3), it becomes clear that the differences are localized. In general, we find that changes in the composition gradient cause shifts in the B-V frequency. Moving across an interface where the gradient becomes steeper, the B-V frequency shifts higher; at an interface where the gradient becomes more shallow, the B-V frequency shifts lower. The greater the change in the gradient, the larger the shift in the B-V frequency.

3.1. *Proof of Concept*

We began by generating a model with the same mass, temperature, helium-layer mass, and internal composition as the best fit from MNW, but using a uniform internal

chemical profile with constant 20:80 C/O out to the 95% mass point. We identified a sequence of 100 shells in this model spanning a range of fractional mass from 0.20 to 0.97 and perturbed the B-V frequency to try to produce a better match to the observations. We parameterized the perturbation as a multiplicative factor applied to the B-V frequency over a range of shells, described by four parameters: (1) the innermost shell to perturb, (2) the magnitude of the perturbation at the innermost shell, (3) the number of shells in the perturbation range, and (4) the magnitude of the perturbation at the outermost shell. These four parameters are sufficient to describe a profile with two abrupt changes in the composition gradient.

The innermost shell was allowed to be any of the 100 shells, and the number of shells in the perturbation range was allowed to be between 0 and 100. If the chosen range would introduce perturbations outside of the sequence of 100 shells, the outermost of these shells was the last to be perturbed. The magnitude of the perturbation was allowed to be a multiplicative factor between 1.0 and 3.0 at both the innermost and outermost perturbed shells and was interpolated linearly in the shells between them.

By using a GA to optimize the perturbation, we can try many random possibilities and eventually find the global best fit with far fewer model evaluations than a full grid of the parameter space. We demonstrated this by introducing a particular perturbation to the model and determining the pulsation periods. Using the same unperturbed model, we then attempted to find the parameters of the perturbation by matching the periods using the GA. In nine out of 10 runs (500 generations of 64 trials), the GA found a first-order solution within two grid points of the input perturbation. Thus, the GA combined with a small (625 point) grid search yields a 90% probability of success for an individual run. By repeating the process several times, the probability of finding the correct answer quickly exceeds 99.9%, even while the number of model evaluations required remains hundreds of times lower than a full grid of the parameter space.

3.2. *Application to GD 358*

Having demonstrated that the method works on calculated model periods, we applied it to the observed pulsation periods of GD 358. We began with a model similar to the new best fit determined from the forward modeling described in § 2, but again using a uniform internal chemical profile (constant 16:84 C/O out to $0.95m/M_*$). After the GA had found the best-fit perturbation for GD 358, we reverse-engineered the corresponding chemical profile.

To accomplish this, we first looked in the unperturbed model for the fractional mass corresponding to the innermost and outermost shells in the perturbation range. We fixed the oxygen abundance to that of the unperturbed model from the center out to the fractional mass of the innermost perturbed shell. The size of the shift in the B-V frequency is determined by how much the composition gradient changes at this point, so we adjusted the oxygen abundance at the fractional mass of the outermost perturbed shell until the change in the gradient produced the required shift. Finally, we fixed the oxygen abundance to that value from the outermost perturbed shell out to a fractional mass of 0.95, where it abruptly goes to zero.

After we found the C/O profile of the best-fit perturbation in this way, we fixed this reverse-engineered profile in the models and performed a new fit from forward modeling with the GA to reoptimize the mass, temperature, helium-layer mass, and central oxygen mass fraction. The B-V curve of the final model differs slightly, of course, from that of the original uniform composition model with the perturbation added. But the approximate internal structure is preserved and leads to a better match to the observed pulsation periods than we could have otherwise found.

4. RESULTS

The calculated periods and period spacings ($\Delta P = P_{k+1} - P_k$) for the best-fit models from the new forward modeling and from the reverse approach are shown in the bottom two panels of Figure 4 along with the data for GD 358. The best-fit models of Bradley & Winget (1994) and MNW are shown in the top two panels for comparison. The data in Figure 4 for the observations and our best-fit models are given in Table 2. Some of the improvement evident in the panels of Figure 4 is certainly due to the fact that we have increased the number of free parameters. To evaluate whether or not the new models represent a significant improvement to the fit, we use the Bayes information criterion (BIC), following Montgomery, Metcalfe, & Winget (2001).

The fit in MNW used $n_p = 3$ completely free parameters, although they also sampled several combinations of two additional parameters. This amounts to a partial optimization in five dimensions. To make a fair prediction of the residuals required to be considered significant, we use

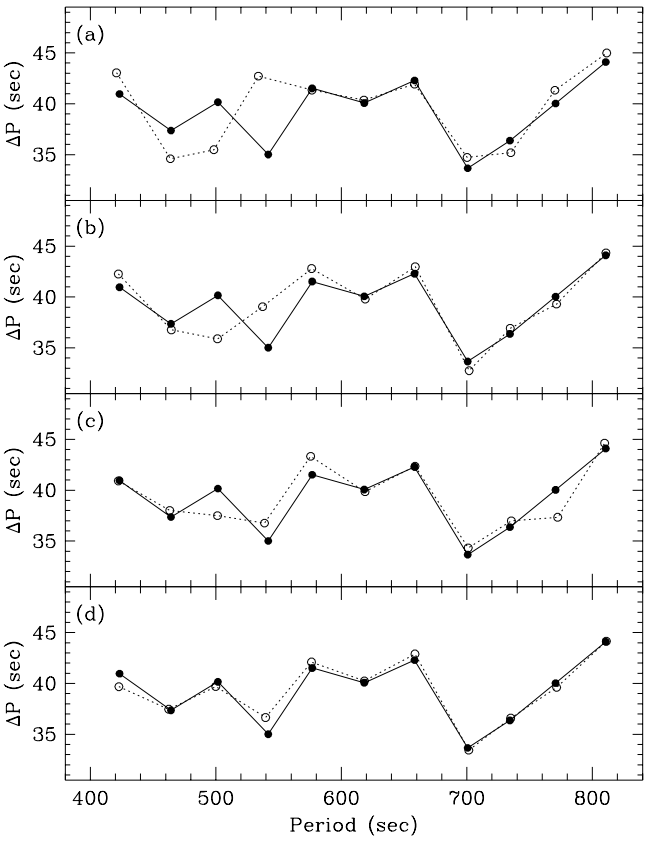

FIG. 4.—Periods and period spacings observed in GD 358 (*filled circles*) with the theoretical best-fit models (*open circles*) from (*a*) Bradley & Winget (1994); (*b*) Metcalfe et al. (2000), (*c*) the new forward modeling presented in § 2, and (d) the reverse approach presented in § 3. Uncertainties on the observations are smaller than the size of the points in this figure.

TABLE 2

PERIODS AND PERIOD SPACINGS FOR GD 358 AND BEST-FIT MODELS

	OBSERVED[a]		MNW FIT[b]		FIVE-PARAMETER FIT		SEVEN-PARAMETER FIT	
k	P	ΔP	P	ΔP	P	ΔP	P	ΔP
8	423.27	40.96	422.31	42.26	422.36	40.92	422.75	39.69
9	464.23	37.36	464.57	36.77	463.28	38.01	462.43	37.46
10.....	501.59	40.16	501.35	35.88	501.29	37.50	499.90	39.70
11.....	541.75	35.01	537.23	39.04	538.79	36.77	539.60	36.65
12.....	576.76	41.52	576.27	42.79	575.56	43.33	576.25	42.10
13.....	618.28	40.07	619.06	39.79	618.89	39.85	618.36	40.25
14.....	658.35	42.29	658.85	42.97	658.74	42.36	658.61	42.90
15.....	700.64	33.66	701.82	32.76	701.10	34.33	701.51	33.44
16.....	734.30	36.37	734.58	36.92	735.42	36.99	734.95	36.59
17.....	770.67	40.03	771.50	39.30	772.41	37.34	771.54	39.60
18.....	810.7	44.1	810.80	44.34	809.75	44.63	811.14	44.15

[a] Winget et al. 1994.
[b] Metcalfe et al. 2000.

their best-fit carbon core model, which represents the best truly three-parameter fit. This model had rms residuals of $\sigma(P) = 2.30$ s for the periods and $\sigma(\Delta P) = 2.65$ s for the period spacings. For $N = 11$ data points, the BIC leads us to expect the residuals of a $n_p = 5$ fit to decrease to $\sigma(P) = 1.84$ s and $\sigma(\Delta P) = 2.13$ s just from the addition of the extra parameters. In fact, the fit from the new forward modeling presented in § 2 has $\sigma(P) = 1.28$ s and $\sigma(\Delta P) = 1.42$ s, so we conclude that the improvement is statistically significant.

The results of the reverse approach presented in § 3 are harder to evaluate because we are perturbing the B-V frequency directly rather than through a specific parameter. We consider each additional point in the internal chemical profile where the composition gradient changes to be a free parameter. Under this definition, the perturbed models are equivalent to a seven-parameter fit, since there are three such points in the profiles, compared to only one for the five-parameter case. If we again use the BIC, we expect the residuals to decrease from their $n_p = 5$ values to $\sigma(P) = 1.03$ s and $\sigma(\Delta P) = 1.14$ s. After reoptimizing the other four parameters using the profile inferred from the reverse approach, the residuals actually decreased to $\sigma(P) = 1.11$ s and $\sigma(\Delta P) = 0.71$ s. The decrease in the period residuals is not significant, but the period spacings are improved considerably. This is evident in the bottom panel of Figure 4.

Adopting the central oxygen mass fraction from the best-fit forward modeling, $X_O = 84 \pm 3$, we can place preliminary constraints on the $^{12}C(\alpha, \gamma)^{16}O$ cross section. Salaris et al. (1997) made detailed evolutionary calculations for main-sequence stellar models with masses between 1 and 7 $M_\odot$ to provide internal chemical profiles for the resulting white dwarfs. For the bulk of the calculations they adopted the rate of Caughlan et al. (1985) for the $^{12}C(\alpha, \gamma)^{16}O$ reaction ($S_{300} = 240$ keV barns), but they also computed an evolutionary sequence using the lower cross section inferred by Woosley, Timmes, & Weaver (1993) from solar abundances ($S_{300} = 170 \pm 50$ keV barns). The chemical profiles from both rates had the same general shape, but the oxygen abundances were uniformly smaller for the lower rate. In both cases the C/O ratio was constant out to the 50% mass point, a region easily probed by white dwarf pulsations.

The central oxygen mass fraction is lower in higher mass white dwarf models. The rate of the triple-α reaction (a three-body process) increases faster at higher densities than does the $^{12}C(\alpha, \gamma)^{16}O$ reaction. As a consequence, more helium is used up in the production of carbon, and relatively less is available to produce oxygen in higher mass models. Interpolating between the models of Salaris et al. (1997), which used the higher value of the cross section, we expect a central oxygen mass fraction for an $M = 0.65\ M_\odot$ model of $X_O^{high} = 0.75$. Using additional calculations for the low rate (M. Salaris 2001, private communication), the expected value is $X_O^{low} = 0.62$. Extrapolating to the value inferred from our new forward modeling, we estimate that the astrophysical S-factor at 300 keV for the $^{12}C(\alpha, \gamma)^{16}O$ cross section is in the range $S_{300} = 290 \pm 15$ keV barns (internal uncertainty only).

The internal chemical profiles corresponding to the best-fit models from §§ 2 and 3 are shown in Figure 5 with the theoretical profile for a 0.61 $M_\odot$ model from Salaris et al. (1997), scaled to a central oxygen mass fraction of 0.80. The profile from the best-fit forward modeling matches the location and slope of the initial shallow decrease in the theoretical profile. The reverse approach also finds significant structure in this region of the model and is qualitatively similar to the Salaris et al. (1997) profile to the extent that our parameterization allows.

5. DISCUSSION AND FUTURE WORK

The extension of the genetic algorithm–based approach to optimize the internal composition and structure of our best-fit white dwarf models to GD 358 has yielded some exciting results. The values of the three parameters considered in the initial study (M_*, $T_{\rm eff}$, $M_{\rm He}$) are unchanged in the full five-parameter fit, so we feel confident that they are the most important for matching the gross period structure. The significant improvement to the fit made possible by including X_O and q as free parameters confirms that the observed pulsations really do contain information about the hidden interiors of these stars.

The efficiency of the GA relative to a grid search is much higher for the larger parameter space, and the ability of the method to find the global best fit is undiminished. The application of this method to data on additional pulsating white dwarfs will help us to assess the significance of our results so we can begin to understand the statistical properties of these ubiquitous and relatively simple stellar objects.

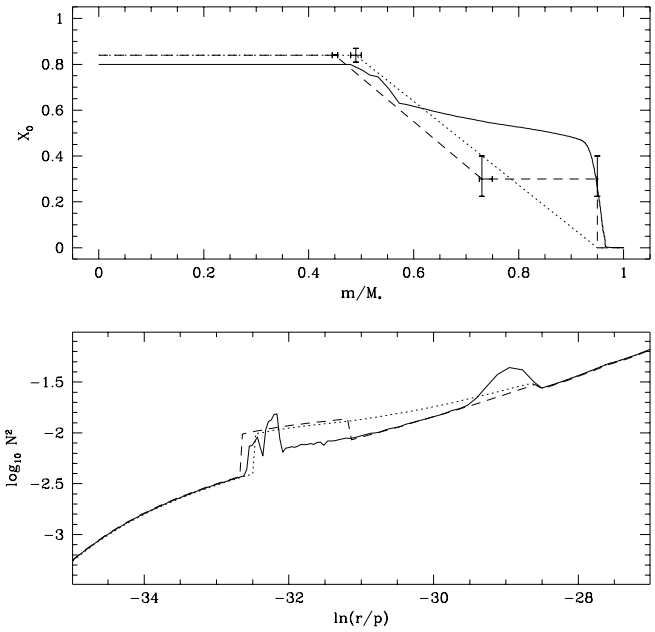

FIG. 5.—Internal oxygen profiles (*top*) and corresponding region of the Brunt-Väisälä curves (*bottom*) for the best-fit forward model from § 2 (*dotted line*), the result of the best-fit reverse approach from § 3 (*dashed line*), and the scaled theoretical calculations of Salaris et al. (1997) for comparison (*solid line*).

It may also provide us with new insights into the processes involved in white dwarf evolution.

Our reverse approach to model fitting was originally motivated by the fact that the variance of our best-fit model from the forward method was still far larger than the observational uncertainties. Although this initial application has demonstrated the clear potential of this approach to yield better fits to the data, the improvement to the residuals was only marginally significant. We will continue to develop this approach, but we must simultaneously work to improve the input physics of our models. In particular, since the internal profile from this initial application is qualitatively similar to the theoretical profiles (given what is possible with this parameterization), we should really include oxygen in our envelopes and eventually calculate fully self-consistent models out to the surface.

Turning the central oxygen abundance into a more precise constraint on the $^{12}C(\alpha, \gamma)^{16}O$ nuclear reaction cross section will require additional detailed simulations like those of Salaris et al. (1997). By determining the range of values for the cross section that produce a central oxygen abundance within the measurement uncertainties of X_O, we should be able to surpass the precision of the extrapolation from laboratory data by nearly an order of magnitude. To assess the systematic uncertainties, we will also need to determine the relative importance of model-dependent details such as convection.

We would like to thank Ed Nather and Mike Montgomery for helpful discussions and M. Salaris for providing us with data files of the theoretical white dwarf internal chemical profiles. We are grateful to the High Altitude Observatory Visiting Scientist Program for fostering this collaboration in a very productive environment for 2 months during the summer of 2000. This work was supported by grant NAG 5-9321 from the Applied Information Systems Research Program of the National Aeronautics and Space Administration, and in part by grant AST 98-76730 from the National Science Foundation.

APPENDIX

At first glance, it may seem that our parameterization of the internal chemical profile might introduce large deviations from the mean period spacing as a result of the abrupt change in the composition gradient. To demonstrate that the models are not

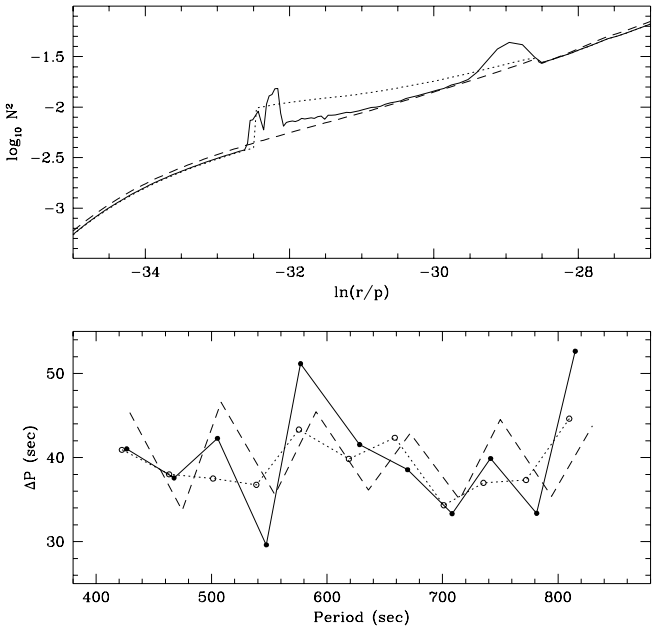

FIG. 6.—Brunt-Väisälä frequency in the region of the models that correspond to the internal chemical profile (*top*) and the period spacing diagrams (*bottom*) for our best-fit forward model from § 2 (*dotted line*), a uniform 20:80 C/O model (*dashed line*), and a scaled theoretical profile from Salaris et al. (1997) for comparison (*solid line*).

unusually sensitive to our profiles when compared to smooth profiles, we calculated the pulsation periods of models with the best-fit parameters from Metcalfe et al. (2000) using several internal chemical profiles. The results are shown in Figure 6. In the top panel, we show the Brunt-Väisälä frequency in the region of the models that correspond to the internal chemical profile. In the bottom panel, we show the period spacing diagrams for each of these models. We find that deviations from the mean period spacing for a model using an internal chemical profile from our parameterization have a magnitude comparable to those caused by a profile with a uniform C/O mixture out to the 95% mass point. The smooth profile from Salaris et al. (1997) causes the largest deviations of the three.

REFERENCES

Arcoragi, J., & Fontaine, G. 1980, ApJ, 242, 1208
Beauchamp, A., Wesemael, F., Bergeron, P., Fontaine, G., Saffer, R. A., Liebert, J., & Brassard, P. 1999, ApJ, 516, 887
Bradley, P. A., & Winget, D. E. 1994, ApJ, 421, 236
Bradley, P. A., Winget, D. E., & Wood, M. A. 1993, ApJ, 406, 661
Buchmann, L. 1996, ApJ, 468, L127
Caughlan, G. R., et al. 1985, At. Data Nucl. Data Tables, 32, 197
Fowler, W. A. 1986, in Highlights of Modern Physics, ed. S. L. Shapiro & S. A. Teukolsky (New York: Wiley), 3
Harrington, R. S., et al. 1985, AJ, 90, 123
Metcalfe, T. S., Nather, R. E., & Winget, D. E. 2000, ApJ, 545, 974 (MNW)
Montgomery, M. H., Metcalfe, T. S., & Winget, D. E. 2001, ApJ, 548, L53
Nather, R. E., Winget, D. E., Clemens, J. C., Hansen, C. J., & Hine, B. P. 1990, ApJ, 361, 309
Salaris, M., Domínguez, I., García-Berro, E., Hernanz, M., Isern, J., & Mochkovitch, R. 1997, ApJ, 486, 413
Tassoul, M., Fontaine, G., & Winget, D. E. 1990, ApJS, 72, 335
Winget, D. E., et al. 1994, ApJ, 430, 839
Wood, M. 1990, Ph.D. thesis, Univ. Texas Austin
Woosley, S. E., Timmes, F. X., & Weaver, T. A. 1993, in Nuclei in the Cosmos, Vol. 2, ed. F. Kappeler & K. Wisshak (Philadelphia: IoP), 531